Potentiation of Cannabinoid-Induced Cytotoxicity in Mantle Cell Lymphoma through Modulation of Ceramide Metabolism

Kristin Gustafsson,[1] Birgitta Sander,[1] Jacek Bielawski,[2] Yusuf A. Hannun,[2] and Jenny Flygare[1]

[1]Department of Laboratory Medicine, Division of Pathology, Karolinska Institutet and Karolinska University Hospital Huddinge, Stockholm, Sweden and [2]Department of Biochemistry and Molecular Biology, Medical University of South Carolina, Charleston, South Carolina

Abstract

Ceramide levels are elevated in mantle cell lymphoma (MCL) cells following treatment with cannabinoids. Here, we investigated the pathways of ceramide accumulation in the MCL cell line Rec-1 using the stable endocannabinoid analogue *R*(+)-methanandamide (R-MA). We further interfered with the conversion of ceramide into sphingolipids that promote cell growth. Treatment with R-MA led to increased levels of ceramide species C_{16}, C_{18}, C_{24}, and $C_{24:1}$ and transcriptional induction of ceramide synthases (CerS) 3 and 6. The effects were attenuated using SR141716A, which has high affinity to cannabinoid receptor 1 (CB1). The CB1-mediated induction of CerS3 and CerS6 mRNA was confirmed using Win-55,212-2. Simultaneous silencing of CerS3 and CerS6 using small interfering RNA abrogated the R-MA-induced accumulation of C_{16} and C_{24}. Inhibition of either of the enzymes serine palmitoyl transferase, CerS, and dihydroceramide desaturase within the *de novo* ceramide pathway reversed ceramide accumulation and cell death induced by R-MA treatment. To enhance the cytotoxic effect R-MA, sphingosine kinase-1 and glucosylceramide synthase, enzymes that convert ceramide to the pro-proliferative sphingolipids sphingosine-1-phospate and glucosylceramide, respectively, were inhibited. Suppression of either enzyme using inhibitors or small interfering RNA potentiated the decreased viability, induction of cell death, and ceramide accumulation induced by R-MA treatment. Our findings suggest that R-MA induces cell death in MCL via CB1-mediated up-regulation of the *de novo* ceramide synthesis pathway. Furthermore, this is the first study were the cytotoxic effect of a cannabinoid is enhanced by modulation of ceramide metabolism. (Mol Cancer Res 2009;7(7):1086–98)

Received 7/31/08; revised 2/18/09; accepted 2/26/09; published 7/16/09.
Grant support: Swedish Cancer Society, Swedish Research Council, Gunnar Nilsson Cancer Foundation, Cancer Society in Stockholm, Magnus Bergvall Foundation, Karolinska Institutet Funds, Stockholm County Council funds, Fernström funds, Swedish Society of Medicine, Boehringer-Ingelheim travel fund, and NIH grant CA87584.
The costs of publication of this article were defrayed in part by the payment of page charges. This article must therefore be hereby marked *advertisement* in accordance with 18 U.S.C. Section 1734 solely to indicate this fact.
Requests for reprints: Jenny Flygare, F-46, Karolinska Sjukhuset Huddinge, SE-14186 Stockholm, Sweden. Phone: 46-8-58581009; Fax: 46-8-58587730. E-mail: jenny.flygare@ki.se

doi:10.1158/1541-7786.MCR-08-0361

Introduction

Ceramide accumulation is a widely described event in cancers after various treatments (1). C_{16}-ceramide is described as one of the major ceramide subspecies, the levels of which are elevated during apoptosis induced by various agents (2). For instance, C_{16} ceramide, generated *de novo*, was accumulated during androgen ablation in the prostate cell line LNCaP (3). Both C_{16} and C_{24} ceramide accumulated during BcR crosslinking in Ramos cells (4, 5). When ceramide species C_{18} was specifically induced in UM-SCC-22A cells (squamous cell carcinoma of hypopharynx) by overexpression of CerS1, cell growth was inhibited (6).

In previous publications (7-9), we and others observed that induction of ceramide accumulation by cannabinoids leads to apoptosis in mantle cell lymphoma (MCL), glioma, and pancreatic cancer. The signaling leading to cell death was blocked by inhibition of ceramide synthase (CerS) with fumonisin B1 (FB1). In MCL, the accumulation of ceramide was mediated through the cannabinoid receptors type 1 (CB1) and type 2 (CB2), which are overexpressed on MCL cells, whereas control cells lacking the receptors remained unaffected.

There are six species of CerS, and several isoforms have been described (2). CerS1 to CerS6 synthesize ceramides of varying chain length (2). When CerS3 was overexpressed in HEK-293T cells, an increased production of C_{18} and C_{24} ceramide species was observed (10), whereas overexpression of CerS6 showed that the enzyme preferably synthesized the long-chain ceramide species C_{14} and C_{16} ceramide (11).

CerS can act through two different pathways, as they are involved in both *de novo* synthesis of (dihydro)ceramide and regeneration of ceramide from sphingosine in the salvage/recycling pathway (see Fig. 1). Several enzymes are involved in the *de novo* synthesis of ceramide, which starts with the precursors L-serine and palmitoyl-CoA. Their conversion into 3-ketosphinganine is catalyzed by serine palmitoyl transferase (SPT; ref. 12). Further downstream, sphinganine is acylated to dihydroceramide by CerS. The dihydroceramide is desaturated by dihydroceramide desaturase (DEGS) to ceramide (13). On the other hand, in the salvage/recycling pathway, CerS act on sphingosine that is generated from the breakdown of complex sphingolipids. Because FB1 inhibits CerS, its actions do not distinguish between the activation of the *de novo* pathway and the operation of the salvage pathway. Thus, it became important to determine the specific pathway activated by cannabinoids.

Once ceramide is synthesized, it can be rapidly metabolized into sphingomyelin, glucosylceramide, or sphingosine (see

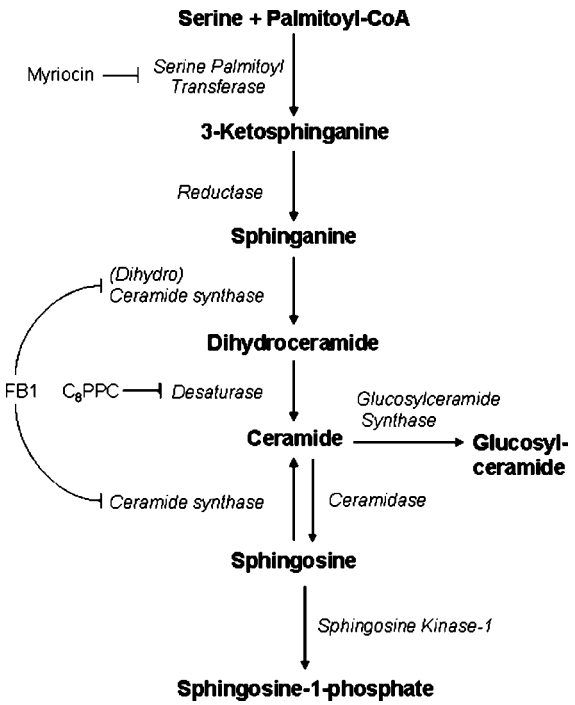

FIGURE 1. Ceramide metabolism. The enzyme ceramide synthase (CerS) can synthesize ceramide from sphingosine in addition to catalyzing the conversion of sphinganine to dihydroceramide within the *de novo* ceramide synthesis pathway. Ceramide can be converted to glucosylceramide by glucosylceramide synthase (GCS) or by sphingosine kinase-1 (SK-1) to sphingosine-1-phosphate (S1P).

Fig. 1), and the latter two can be further converted to complex glycosphingolipids or sphingosine-1-phosphate (S1P), respectively. Metabolism of active ceramide into such species by glucosylceramide synthase (GCS) or sphingosine kinase-1 (SK-1) is the limiting factor in the cell death response to ceramide-inducing stimuli (1). It has been shown in multiple cell types (14) that manipulating ceramide metabolism by blocking enzymes leads to a potentiation of cell death. Also, the balance between ceramide and S1P is vital to the cell death decision in many cancer types (15, 16). Safingol, an inhibitor of SK-1, has been shown to synergistically increase the efficacy of the cytotoxic drug fenretinide in neuroblastoma cells (17). Down-regulation of SK-1 by actinomycin D in Molt-4 cells has been shown to decrease viability and induce cell death (18). Resistant melanoma cells Mel-2a showed increased rate of apoptosis after treatment with small interfering RNA (siRNA) against SK-1 together with Fas antibody CH-11 or C_6-ceramide (19). Several studies have shown that overexpression of GCS in cancers can generate multidrug resistance caused by subsequent up-regulation of the multidrug resistance 1 gene (20, 21). There are multiple publications stating that GCS inhibitors (e.g., PDMP, PPMP, and PPPP) can enhance the effect of chemotherapeutic drugs in resistant cells (22, 23). Using antisense to down-regulate GCS in resistant breast cancer cells, MCF-7/Adr, Gouaze et al. (24) showed a decrease in multidrug resistance 1 expression leading to an increased cell death by vinblastine.

In our previous publications, we have induced cell death by treatment of lymphoma cells with different cannabinoids *in vitro* (7, 25) and observed a 40% reduction of tumor burden in NOD/SCID mice xenotransplanted with human MCL by treatment with the stable endocannabinoid analogue *R*(+)-methanandamide (R-MA) *in vivo* (7). These results, together with those implicating ceramide in the action of cannabinoids, raised the possibility that preventing the transformation of ceramide into other forms of sphingoplipids could enhance the cell death response in MCL. Further, the Nordic Lymphoma Network reported that adding the chemotherapeutic agents doxorubicin and 1-β-D-arabinofuranosylcytosine, both inducers of ceramide accumulation, to MCL treatment has improved the event-free survival for MCL patients (26). Thus, ceramide accumulation appears to contribute to the reduction of malignant MCL cells *in vivo*.

In this study, we investigated the mechanisms and specificity of the ceramide response to R-MA. We further exploited this understanding to determine if modulating ceramide levels could potentiate the cytotoxic response to R-MA. The obtained data show that R-MA treatment leads to increased expression of CerS, *de novo* synthesis of specific ceramide species, and apoptosis in the MCL cell line Rec-1. Modulation of ceramide metabolism using inhibitors or RNA interference potentiates the apoptosis-inducing effect of R-MA.

Results

Treatment with Methanandamide Induces Accumulation of Different Ceramide Species in MCL

We have previously shown that treatment of MCL cells with cannabinoids leads to an accumulation of ceramide (7). The effect was mediated by the cannabinoid receptors CB1 and CB2. To further study the time course of ceramide accumulation, the MCL cell line Rec-1 was treated with 10 μmol/L R-MA, and total [^{3}H]ceramide was analyzed using tritium labeling and liquid scintillation. After 30 min of treatment, only a slight increase in [^{3}H]ceramide accumulation was observed compared with the mock-treated control. After 4 h, there was a 30% increase in the accumulation of [^{3}H]ceramide, which was even more pronounced after 12 or 24 h (Fig. 2).

The induction of ceramide in MCL is dependent of signaling via the CB1 receptor (7). To investigate the accumulation of different ceramide species, Rec-1 cells, which express the CB1 receptor, were treated with increasing doses of R-MA. As a control, the cell line SK-MM, which has higher endogenous levels

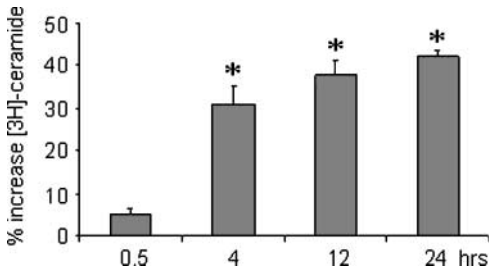

FIGURE 2. Time course of the accumulation of total ceramide in response to R-MA. MCL cell line Rec-1 was labeled with [^{3}H]palmitic acid followed by treatment with 10 μmol/L R-MA for 30 min, 4 h, 12 h, and 24 h. Tritiated ceramide was evaluated by liquid scintillation spectroscopy as detailed in Materials and Methods. [^{3}H]ceramide was normalized against the total number of ^{3}H-labeled cells loaded per sample. One of three individually performed experiments. *, $P < 0.05$, R-MA-treated cells compared with vehicle-treated control cells at the same time point (Kruskal-Wallis analysis).

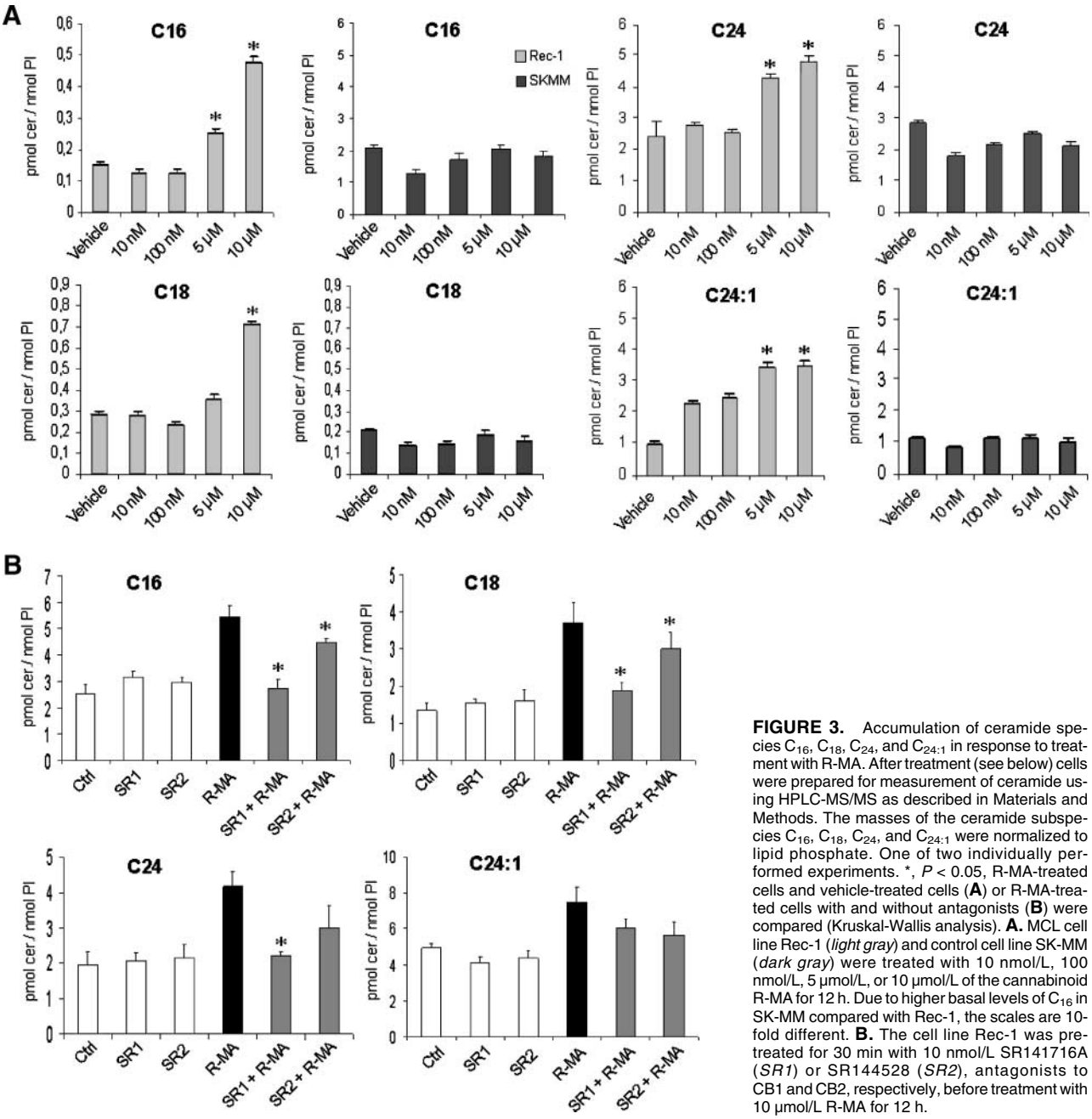

FIGURE 3. Accumulation of ceramide species C_{16}, C_{18}, C_{24}, and $C_{24:1}$ in response to treatment with R-MA. After treatment (see below) cells were prepared for measurement of ceramide using HPLC-MS/MS as described in Materials and Methods. The masses of the ceramide subspecies C_{16}, C_{18}, C_{24}, and $C_{24:1}$ were normalized to lipid phosphate. One of two individually performed experiments. *, $P < 0.05$, R-MA-treated cells and vehicle-treated cells (**A**) or R-MA-treated cells with and without antagonists (**B**) were compared (Kruskal-Wallis analysis). **A.** MCL cell line Rec-1 (*light gray*) and control cell line SK-MM (*dark gray*) were treated with 10 nmol/L, 100 nmol/L, 5 μmol/L, or 10 μmol/L of the cannabinoid R-MA for 12 h. Due to higher basal levels of C_{16} in SK-MM compared with Rec-1, the scales are 10-fold different. **B.** The cell line Rec-1 was pretreated for 30 min with 10 nmol/L SR141716A (*SR1*) or SR144528 (*SR2*), antagonists to CB1 and CB2, respectively, before treatment with 10 μmol/L R-MA for 12 h.

of ceramide C_{16} but lacks CB1 expression, was used. The cell lines were treated for 12 h with R-MA, and the levels of ceramide species were measured by high-performance liquid chromatography-tandem mass spectrometry (HPLC-MS/MS). A 2- to 3.5-fold increase of ceramide species C_{16}, C_{18}, C_{24}, and $C_{24:1}$ was observed when the MCL cell line Rec-1 was treated with 5 or 10 μmol/L R-MA, whereas lower doses had no effect (Fig. 3A). The levels of ceramide species C_{14}, C_{20}, C_{22}, $C_{22:1}$, C_{26}, and $C_{26:1}$ remained unaltered (data not shown). No accumulation of any of the ceramide species was observed after stimulation of the control cell line SK-MM with R-MA (Fig. 3A). These results show that R-MA induced a subset of ceramide species specifically in MCL. Pretreatment with SR141716A, an antagonist with high affinity for CB1, significantly prevented the accumulation of ceramide species C_{16}, C_{18}, and C_{24}, whereas SR144528, which binds to CB2, partially inhibited the accumulation of C_{16} and C_{18} (Fig. 3B). These results indicate that R-MA causes accumulation of specific ceramide species mainly via the CB1 receptor.

Methanandamide Treatment Induces Selective Up-Regulation of CerS3 and CerS6 in Rec-1 Cells

The relatively late increase in total ceramide levels following treatment with methanandamide raised the possibility that

transcriptional up-regulation of the CerS could contribute to the accumulation of ceramide. Therefore, Rec-1 cells and SK-MM cells were treated with 10 μmol/L R-MA (Fig. 4A, *top*) for 12 h, and the expression of CerS was investigated by quantitative real-time PCR. In Rec-1, CerS3 and CerS6 showed 2- and 2.6-fold increase of expression, respectively, after R-MA treatment. In contrast, CerS1 variant 2 showed decreased expression, whereas the expressions of CerS1 variant 1, CerS2, CerS4, and CerS5 were only marginally altered (Fig. 4A, *top*). There was no substantial increase in the expression of CerS in the control cell line SK-MM. These results were confirmed using 10 μmol/L of the synthetic cannabinoid Win-55,212-2 (Win-55; Fig. 4A, *bottom*). When Rec-1 cells were pretreated with 10 nmol/L SR141716, the induction of CerS3 and CerS6 was inhibited to a large extent (Fig. 4B). SR144528 caused a partial inhibition of the R-MA-induced up-regulation of CerS3, whereas the attenuation of the induction of CerS6 in response to R-MA and of both CerS in response to Win-55 was not significant (Fig. 4B).

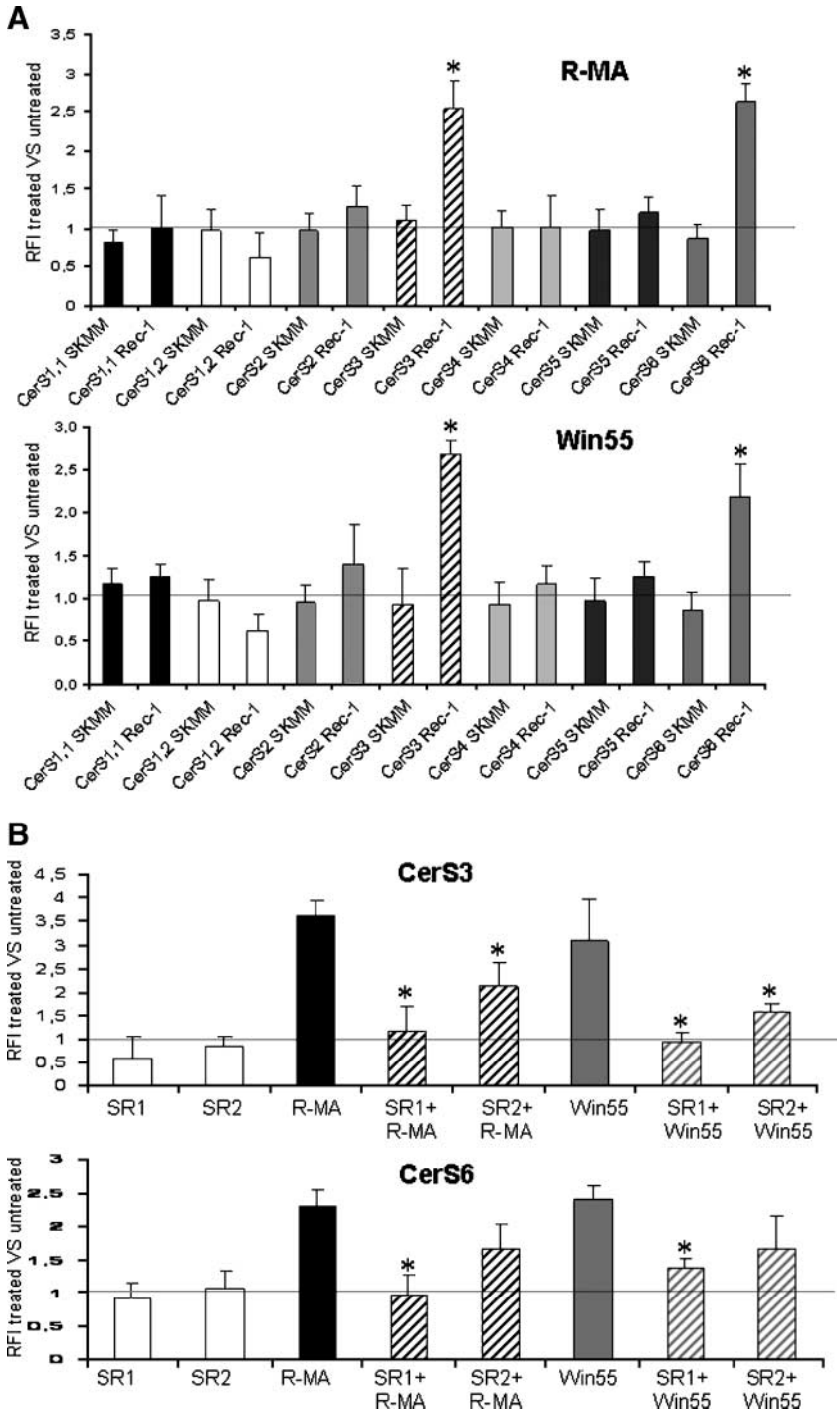

FIGURE 4. Expression of CerS after cannabinoid treatment. **A.** MCL cell line Rec-1 and control cell line SK-MM were treated for 12 h with 10 μmol/L R-MA (*top*) or Win-55 (*bottom*). **B.** Rec-1 cells were pretreated with 10 nmol/L SR141716 or SR144528, antagonists to CB1 and CB2, respectively, before treatment with 10 μmol/L R-MA or Win-55 for 12 h. After treatment, CerS was detected by quantitative PCR. Relative fold increase (*RFI*) in the expression of CerS in treated samples compared with control samples. All samples were normalized to the reference gene β-actin. *, $P < 0.05$, R-MA-treated cells and vehicle-treated cells (**A**) with and without antagonists (**B**) were compared (Kruskal-Wallis analysis).

To investigate if the up-regulation of CerS following treatment with R-MA gave rise to increased accumulation of ceramides, Rec-1 cells were transfected with siRNA against CerS3 and CerS6. No change in accumulation of ceramide subspecies was observed when either enzyme was silenced. However, when both CerS3 and CerS6 were knocked down simultaneously, the accumulation of ceramide species C_{16} and C_{24} was abrogated (Fig. 5A). Thus, CerS3 and CerS6 together appear to contribute to part of the earlier observed synthesis of ceramide species (Fig. 3) in response to treatment with R-MA. Similarly, suppression of both CerS3 and CerS6 caused a reproducible, but nonsignificant, decrease in the cell death induced by 10 μmol/L R-MA (Fig. 5B).

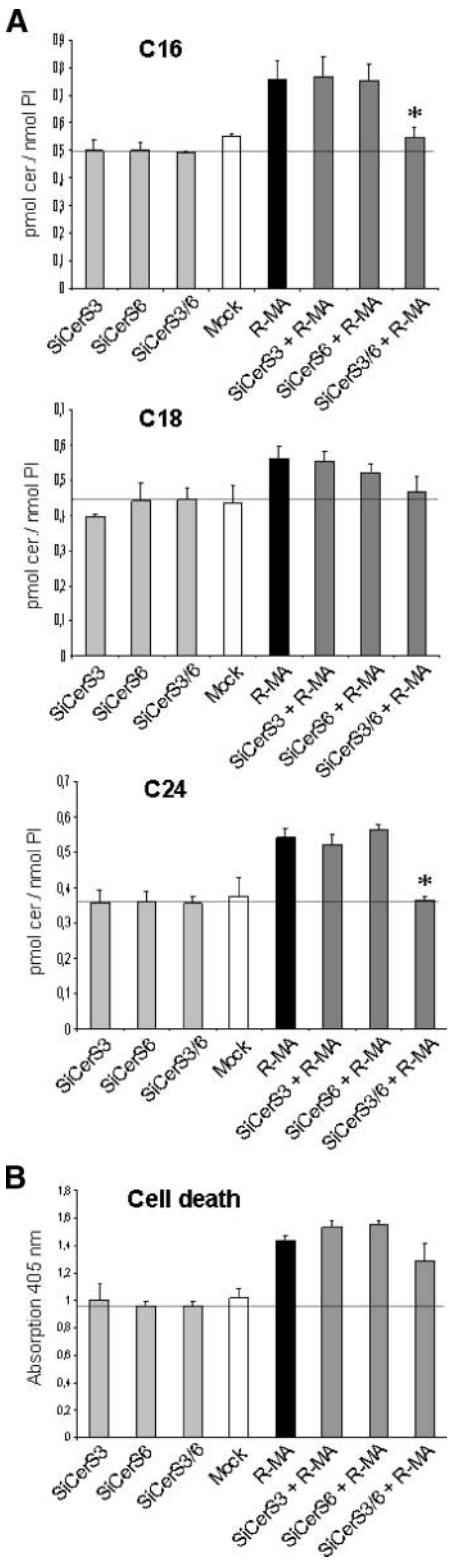

FIGURE 5. **A.** Rec-1 cells were transfected with siRNA against CerS3 and CerS6. After 24 h, 10 μmol/L R-MA was added for 12 h. Measurement of ceramide using HPLC-MS/MS was done as described in Materials and Methods. The masses of the ceramide subspecies C_{16}, C_{18}, C_{24}, and $C_{24:1}$ were normalized to lipid phosphate. *, $P < 0.05$, R-MA-treated cells with and without siRNA were compared (Kruskal-Wallis analysis). **B.** Rec-1 cells were transfected with siRNA against CerS3 and/or CerS6 for 24 h and subsequently treated with 10 μmol/L R-MA for 12 h. Thereafter, the Cell Death ELISA was done. *Y axis,* fluorescence units. One of two individually performed experiments.

Inhibition of Enzymes in the De novo *Ceramide Pathway Leads to Decreased Ceramide Accumulation and Decreased Cell Death in Response to R-MA Treatment*

To delineate the pathway leading to synthesis of ceramide after stimulation with R-MA, inhibitors targeting enzymes in the *de novo* pathway were used. Cells were labeled with radioactive tritium and pretreated with myriocin, FB1, or C_8-cyclopropenylceramide (C_8-CPPC), inhibitors to SPT, CerS, and DEGS, respectively (refs. 27-29; Fig. 1), before treatment with 10 μmol/L R-MA. The formation of ceramide was disrupted following pretreatment with each of these inhibitors (Fig. 6), strongly suggesting that ceramide was synthesized through the *de novo* pathway and not from the salvage pathway. The study was extended by analyzing different ceramide species using HPLC-MS/MS. After treatment with inhibitors and R-MA as described above, accumulation of ceramide species C_{16}, C_{18}, C_{24}, and $C_{24:1}$ was abrogated (Fig. 7).

To examine the role of *de novo* ceramide synthesis in the induction of apoptosis, cell death was estimated using Cell Death ELISA and Annexin V/propidium iodide staining combined with flow cytometry. Rec-1 cells were preincubated with myriocin, FB1, or C_8-CPPC before treatment with 10 μmol/L R-MA. When *de novo* synthesis was disrupted, apoptosis induced by R-MA was abrogated (Fig. 8A and B). Because these inhibitors act at different stages of the *de novo* pathway, the results show that ceramide (or downstream metabolites) and not dihydroceramide or other upstream metabolites in the *de novo* pathway is the primary mediator. This confirms and extends our previous observations that FB1, an inhibitor of CerS, abrogated the induction of cell death.

Suppression of Ceramide-Metabolizing Enzymes Using Inhibitors or siRNA Potentiates to the Decreased Viability, Increased Cell Death, and Ceramide Accumulation Induced by R-MA

It has been shown in earlier studies (30) that increasing ceramide levels by manipulating ceramide metabolism can sensitize cells to cytotoxic treatment. To enhance the targeted cell death induced by cannabinoids in MCL (7), we combined the

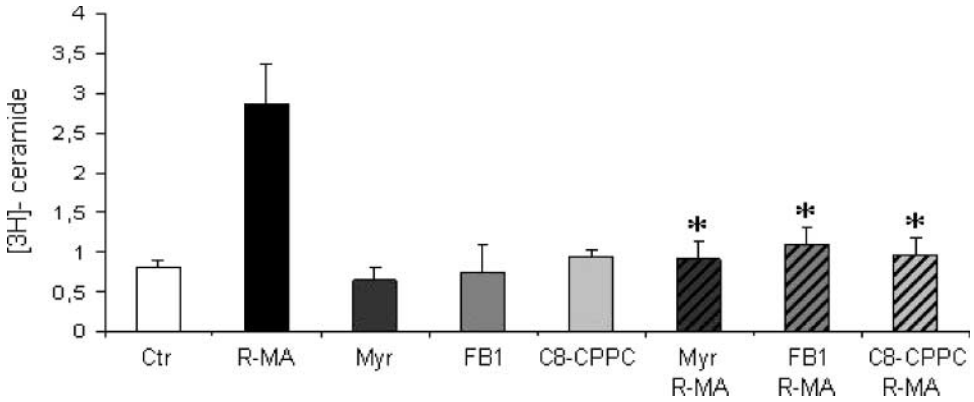

FIGURE 6. Inhibition of enzymes in the *de novo* synthesis pathway before treatment with R-MA leads to disrupted ceramide synthesis. Rec-1 cells were pretreated for 1 hr with 1 μmol/L myriocin, for 1 hr with 25 μmol/L FB1 or for 6 h with 500 nmol/L C_8-CPPC before treatment with 10 μmol/L R-MA for 12 h. Before treatment, the cells were labeled with [^{3}H]palmitic acid. After treatment [^{3}H]ceramide was evaluated by liquid scintillation spectroscopy as detailed in Materials and Methods. [^{3}H]ceramide was normalized against the total number of ^{3}H-labeled cells loaded per sample. One of two individually performed experiments. *, $P < 0.05$, agonist-treated cells with and without inhibitors were compared (Kruskal-Wallis analysis).

R-MA treatment with inhibition of two ceramide-metabolizing enzymes, SK-1 and GCS. Rec-1 cells were cotreated with 10 μmol/L R-MA and the SK-1 inhibitor SKI II or DMS, and after 72 h, viability was examined by XTT. Cotreatment with SKI II (Fig. 9A, *top left*) or DMS (Fig. 9A, *top right*) potentiated the effect of R-MA on its own. Cotreatment with the GCS inhibitors C_9DGJ (Fig. 9A, *bottom left*) and PDMP (Fig. 9A, *bottom right*) had a similar effect. To confirm that the effects observed using the inhibitors of ceramide metabolism in MCL cells were specific, SK-1 and GCS were silenced using siRNA. Rec-1 cells were transfected with 20 nmol/L siRNA duplexes binding to either enzyme before treatment with 10 μmol/L R-MA. siRNA against SK-1 or GCS potentiated the decrease in viability induced by R-MA alone (Fig. 9B).

To determine the effect of inhibitors to ceramide metabolism in combination with 10 μmol/L R-MA on induction of apoptosis, Cell Death ELISA was done. C_9DGJ was used in this experiment because it is more specific to GCS than PDMP (31). SKI II was used because French et al. (32) showed that it specifically inhibits the formation of S1P. Rec-1 cells were cotreated as above and analyzed after 12 h. In accordance with the decrease in viability, there was a potentiation of cell death when SKI II or C_9DGJ was combined with 10 μmol/L R-MA (Fig. 10A). The potentiation was confirmed using siRNA against SK-1 and GCS (Fig. 10B). Taken together, these results show that inhibition of the transformation of ceramide into S1P or glucosylceramide potentiates the viability-suppressing and cell death-inducing effects of R-MA.

To investigate which ceramide species are converted by SK-1 and GCS in Rec-1, siRNA against each enzyme was used in combination with R-MA. Significantly increased levels of ceramide specie C_{16} were detected when SK-1 was inhibited by siRNA against SK-1 before treatment with R-MA (Fig. 11A, *left*), whereas the levels of C_{18} remained unaffected (Fig. 11A, *right*). Cotreatment with R-MA and siRNA against GCS induced significantly increased levels of both ceramide C_{16} and C_{18} (Fig. 11B). No change in the levels of C_{24} or $C_{24:1}$ was observed (data not shown). Thus, inhibition of SK-1 or GCS is likely to potentiate cell death in Rec-1 via R-MA-induced accumulation of C_{16} or C_{16} and C_{18}, respectively.

Discussion

Ceramide is known to function as a second messenger in different cellular processes (e.g., induction of apoptosis and differentiation), and its accumulation can be induced by a variety of stimuli (16). Cannabinoids have been shown to induce ceramide accumulation in pancreatic cancer, glioma, and leukemia cell lines (8, 9, 33) as well as in MCL (7). The production of ceramide following treatment with cannabinoids can be caused by either hydrolysis of sphingomyelin or *de novo* ceramide synthesis (34, 35). In the current study, we have shown accumulation of ceramide species C_{16}, C_{18}, C_{24}, and $C_{24:1}$ in the MCL cell line Rec-1 after long-term stimulation with the stable endocannabinoid analogue R-MA. Ceramides exhibit a tissue-dependent bias for amide-linked fatty acids, characterized by chain length, degree of saturation, and degree of hydroxylation. C_{16} ceramide is known to be most abundant in fibroblasts, endothelial cells, and immune cells (36, 37). In accordance with the present study using a cell line of B-cell origin, C_{16} and C_{24} ceramide species were accumulated after BcR crosslinking in the B-cell line Ramos (4, 5).

It has been shown previously that cannabinoids can induce apoptosis via *de novo* synthesis in C6 glioma cells (35). In the same study, increased activity of SPT was the rate-limiting step in ceramide synthesis *de novo* (38). Here, we observed up-regulation of messages for CerS within the same pathway. The six known forms of CerS are active in two processes, acylating either dihydrosphingosine to form dihydroceramide or sphingosine to form ceramide. After stimulation with R-MA, the Rec-1 cells overexpressed CerS3 and CerS6 2 and 2.6 times, respectively. CerS6 is a major CerS that is expressed at high levels in a variety of tissues (11) and is associated with synthesis of ceramide species C_{14} and C_{16}. CerS3 is regarded as a minor CerS that has mainly been described in skin and testis (10, 39) and has been shown to synthesize the longer ceramide species C_{18}, C_{20}, and C_{24} (10, 11). The induction of CerS3 after stimulation with cannabinoids is intriguing, because database searches show that CerS3 expression is rarely present in lymphoma tissue, whereas CerS6 expression is present in a majority of the lymphomas (Omnibus GEO database).

Silencing of either CerS3 or CerS6 using siRNA had no effect, whereas simultaneous knockdown decreased the accumulation of C_{16}, C_{18}, and C_{24}. Our results suggest that CerS3 and CerS6 may have redundant functions in the production of ceramide species and indicate that CerS6 and CerS3 are not restricted to the synthesis of C_{14} and C_{16} or longer ceramide species, respectively. The contemporaneous suppression of CerS3 and CerS6 had a reproducible, but nonsignificant, inhibitory effect on R-MA-induced cell death. Only two of the four ceramide species that were induced by R-MA were significantly affected by simultaneous suppression of CerS3 and CerS6, and additional CerS, CerS2 and CerS5, showed slightly increased levels following R-MA treatment (Fig. 4A). Moreover, it cannot be excluded that suppression of two CerS may cause compensatory

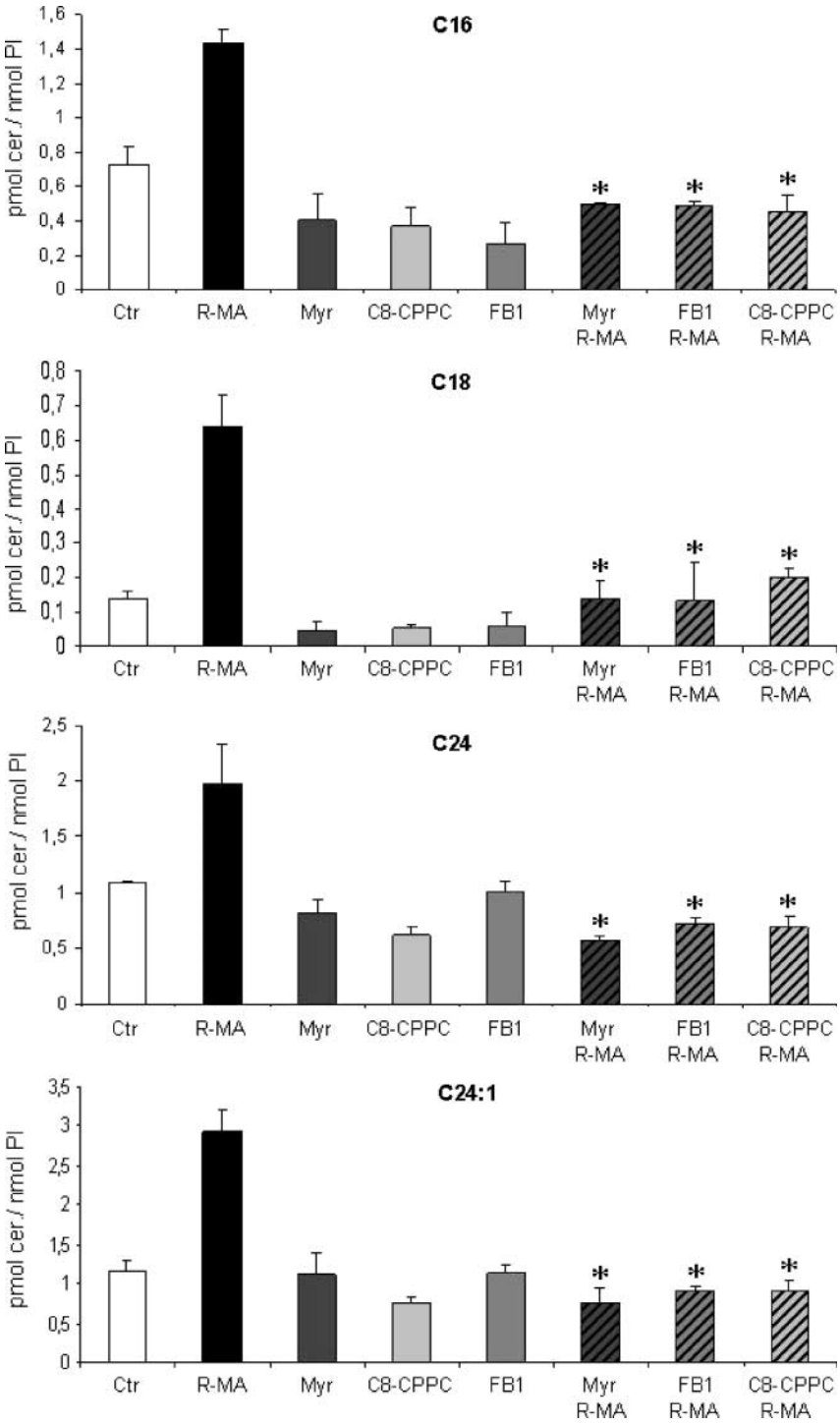

FIGURE 7. Inhibition of the enzymes in the *de novo* synthesis pathway before treatment with R-MA leads to disrupted synthesis of ceramide species. Rec-1 cells were pretreated for 1 h with 1 μmol/L myriocin, for 1 h with 25 μmol/L FB1, or for 6 h with 500 nmol/L C_8–CPPC before treatment with 10 μmol/L R-MA for 12 h. Cells were prepared for measurement using HPLC-MS/MS as described in Materials and Methods. The masses of the ceramide subspecies C_{16}, C_{18}, C_{24}, and $C_{24:1}$ were normalized to lipid phosphate. *, $P < 0.05$, agonist-treated cells with and without inhibitors were compared (Kruskal-Wallis analysis).

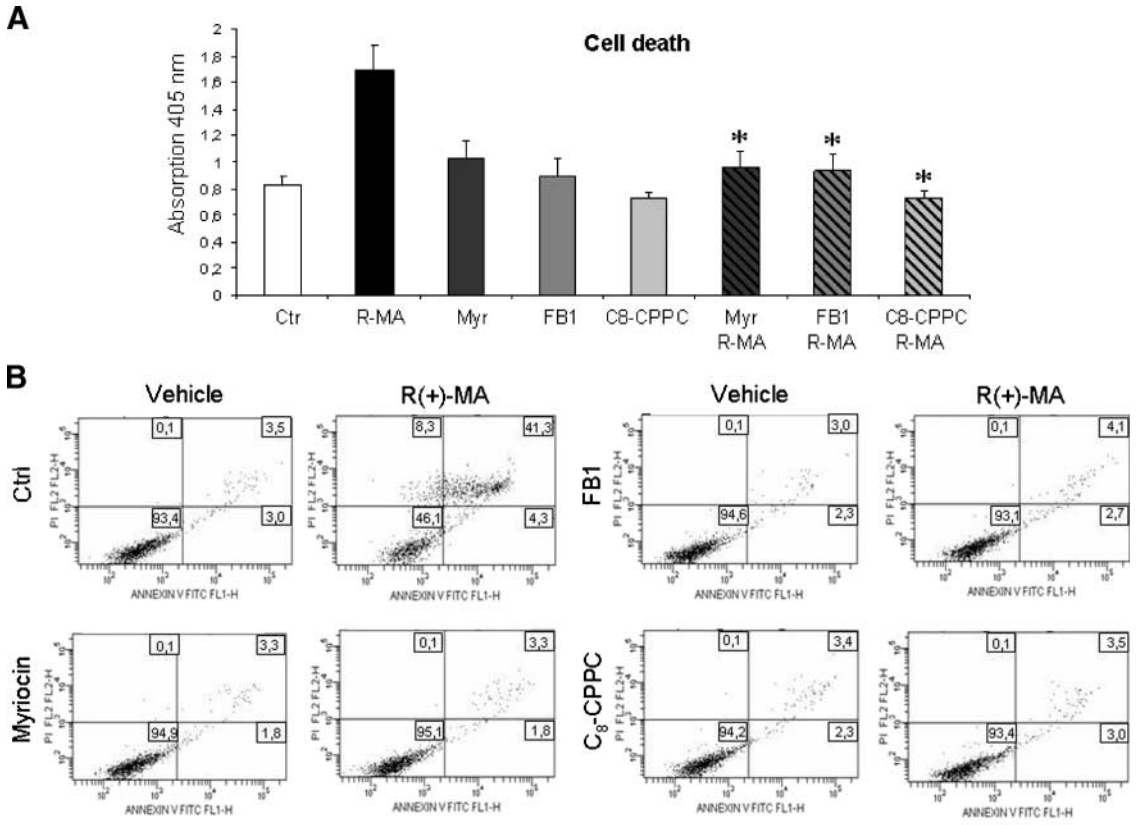

FIGURE 8. Inhibition of enzymes in the *de novo* ceramide synthesis pathway before treatment with R-MA leads to disrupted cell death. Rec-1 cells were pretreated for 1 h with 1 μmol/L myriocin, 1 h with 25 μmol/L FB1, or 6 h with 500 nmol/L C_8-CPPC followed by treatment with 10 μmol/L R-MA for 12 h. **A.** Cell Death ELISA was done. *Y axis*, fluorescence units. One of two individually performed experiments. *, $P < 0.05$, agonist-treated cells with and without inhibitors were compared (Kruskal-Wallis analysis). **B.** Flow cytometry analysis of Annexin V/FITC and propidium iodide. *Top* and *bottom right quadrants,* late apoptotic/necrotic and early apoptotic cells, respectively. Representative results from three individual experiments.

up-regulation of others. Thus, the results indicate that up-regulation of CerS3 and CerS6 contributes to, but does not completely account for, the synthesis of ceramide and subsequent cell death.

The CB1 antagonist SR141716 completely inhibited the R-MA-induced accumulation of ceramide species C_{16}, C_{18}, and C_{24} and the up-regulation of CerS3 and CerS6 following treatment with R-MA or Win-55. SR144528, an antagonist to CB2, partially inhibited the increase in C_{16}, C_{18}, and CerS3, whereas the inhibitory effects on the accumulation of other ceramide species and on the up-regulation of CerS6 were not significant. Given the selectivity of R-MA toward CB1, it may seem surprising that SR144528 counteracted the induction of ceramide accumulation and the up-regulation of CerS. These results are in accordance with our earlier studies showing that antagonists to either CB1 or CB2 attenuated cell death induced by R-MA in MCL and other lymphomas expressing both receptors (7, 40). At the doses used, it is possible that R-MA acts as an agonist also to CB2 despite its much higher affinity to CB1. Alternatively, the binding of SR144528 to CB2 induces changes downstream of the receptor that affect the signaling via CB1.

We have previously blocked cell death in Rec-1 cells by inhibiting CerS with FB1 (7). The same inhibitor has been used to prevent induction of ceramide accumulation by cannabinoids in glioma cells (41). However, CerS can act in two pathways: both in regeneration of ceramide from sphingosine and in *de novo* synthesis (see Fig. 1). To exclude the involvement of SL degradation, we here added inhibitors to enzymes that are active only in the *de novo* pathway: SPT and DEGS. Dbaibo et al. (42) have shown that inhibition of SPT with myriocin abrogates cell death induced by arsenic trioxide in T-cell leukemia and lymphoma. In the present study, inhibition of either of three different enzymes, SPT, CerS, and DEGS, led to an abrogation of ceramide accumulation and suppression of cell death in MCL (Fig. 1). This fortifies the role of *de novo* synthesis in the responses to R-MA.

It has previously been suggested that ceramide is the active mediator of apoptosis, whereas dihydroceramide is merely an inactive precursor to ceramide (14). In these studies, exogenous ceramide and dihydroceramide have been added to cells or mitochondria (43, 44). In contrast, high levels of dihydroceramide were observed in HL-60 leukemia cells before cell death (45), and SMS-KCNR cells were cell cycle arrested when DEGS was inhibited (46). In our MCL cells, the inhibition of DEGS using C_8-CPPC caused accumulation of dihydroceramide species (data not shown) and inhibited the induction of cell death by R-MA. This supports the theory that dihydroceramide species cannot induce apoptosis when the transformation to ceramide is inhibited.

The above conclusion on the central role of ceramide suggested that the cell death-promoting effects of R-MA could be enhanced by inhibiting the transformation of ceramide into species with opposing effects. Inhibition of both SK-1 and GCS potentiated the effects of R-MA on viability and cell death. French et al. (32) have shown that SKI II is a specific inhibitor to S1P formation, which also inhibits tumor growth *in vivo*. In view of the significant potentiation of the R-MA-induced effects observed using SKI II *in vitro*, future *in vivo* studies using a combination of R-MA and SKI II in mice xenotransplanted with MCL cells are warranted. To be assured that the effects observed in our experiments were enzyme specific, GCS and SK-1 were silenced using siRNA. In addition to potentiation of the effects induced by R-MA, silencing of SK-1 led to a decrease in cell viability by itself. Taha et al. (18) and Sarkar et al. (47) have observed that down-regulation of SK-1 by siRNA in MCF-7 cells resulted in a reduction of cell viability. Interference with GCS RNA has also been shown to affect growth of neuroblastoma (23) and sensitize breast carcinoma cells to cytotoxic drugs (21). However, the viability of an astrocytoma cell line following treatment with the cannabinoid Δ9-tetrahydrocannabinol was not affected by inhibitors or siRNA against GCS (48). In our cells, knockdown of SK-1 led to significant potentiation of R-MA-induced C_{16} accumulation, whereas the accumulation of both C_{16} and C_{18} was potentiated using siRNA against GCS. Instead, the levels of C_{24} and $C_{24:1}$ remained unaltered. It is possible that these ceramide species are metabolized by other ceramide-converting enzymes (e.g., sphingomyelin synthase or ceramide kinase; ref. 1).

In conclusion, we have shown that induction of CerS regulates *de novo* ceramide synthesis in response to the stable endocannabinoid analogue R-MA in MCL cells. The effect of inhibition of DEGS supports earlier studies showing that ceramide, and not dihydroceramide, is the active mediator of apoptosis. Moreover, inhibition of enzymes that convert ceramide to growth-promoting sphingolipid species potentiated the ceramide accumulation and cell death induced by R-MA in MCL. Cannabinoids have been suggested as a new nontoxic therapeutic option for cancer treatment (49). This is the first study showing that the cytotoxic effect of a cannabinoid can be enhanced by modulation of ceramide metabolism. The results suggest that interference with ceramide conversion may provide a tool to enhance the targeted cell death-promoting effects of cannabinoids in MCL and other malignant lymphomas overexpressing the CB1 receptor.

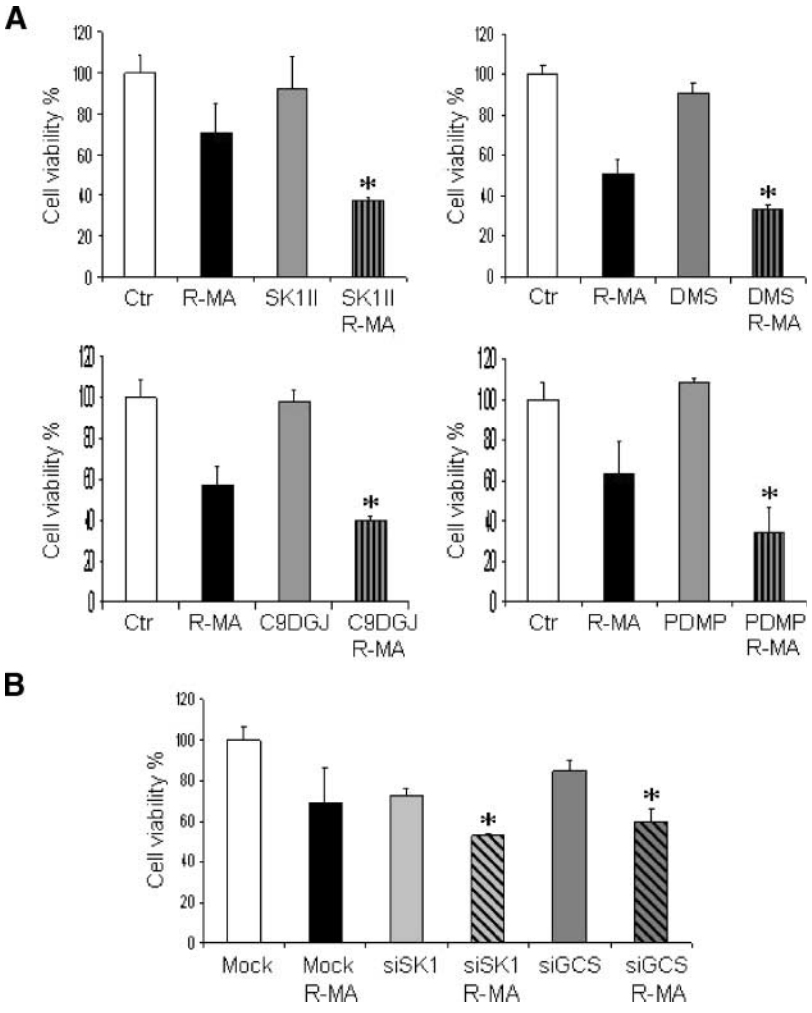

FIGURE 9. Inhibition of ceramide metabolism potentiates reduction of viability induced by R-MA. Following treatment (see below), viability of treated cells is expressed as percent of vehicle-treated control. One of three individually performed experiments. *, $P < 0.05$, agonist-treated cells with and without inhibitors were compared (Kruskal-Wallis analysis). **A.** Rec-1 cells were treated with 10 μmol/L R-MA in combination with 500 nmol/L SKI II, 1 μmol/L DMS (SK-1 inhibitors), 10 μmol/L C_9DGJ, or 10 μmol/L PDMP (GCS inhibitors) for 12 h. XTT assay was done 72 h after treatment. **B.** Rec-1 cells transfected with siRNA against SK-1 or GCS for 24 h were subsequently treated with 10 μmol/L R-MA for 12 h after transfection. Cells were cultured for 48 h before XTT assay was done.

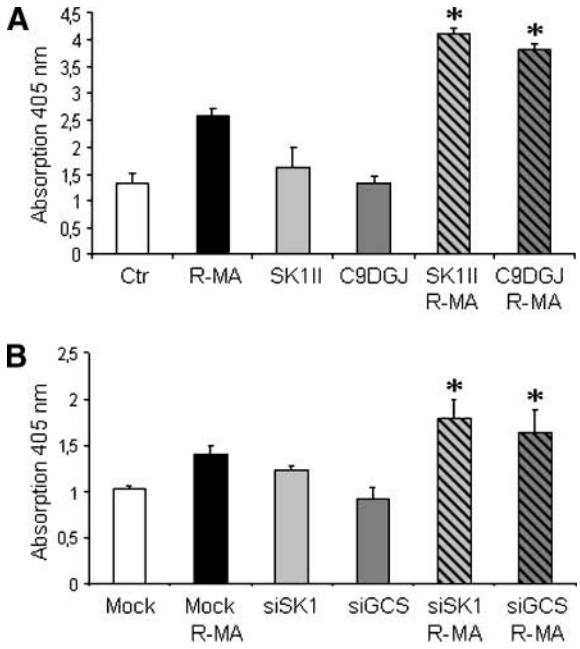

FIGURE 10. Inhibition of ceramide metabolism potentiates cell death induced by R-MA. After treatment (see below), the Cell Death ELISA was done. *Y axis,* fluorescence units. One of two individually performed experiments. *, $P < 0.05$, agonist-treated cells with and without inhibitors or siRNA were compared (Kruskal-Wallis analysis). Rec-1 cells were (**A**) treated with 10 μmol/L R-MA in combination with 500 nmol/L SKI II (SK-1 inhibitor) or 10 μmol/L C_9DGJ (GCS-inhibitor) for 12 h or (**B**) transfected with siRNA against SK-1 or GCS for 24 h and subsequently treated with 10 μmol/L R-MA for 12 h.

Materials and Methods

Reagents and Drugs

R-MA, Win-55, FB1, myriocin, SKI II, DMS, and PDMP were purchased from Sigma-Aldrich Sweden. C_8-CPPC was obtained from Matreya. ^{3}[H]palmitate was purchased from Amersham Biosciences. siRNA duplexes against CerS3, CerS6, GCS, and SK-1 were purchased from Ambion and diluted to 200 nmol/L in siRNA dilution buffer (Qiagen). AIM-V medium was purchased from Invitrogen.

Cell Lines

The MCL cell line Rec-1 was a kind gift from Dr. Christian Bastard, Ronan, France. The plasma cell line SK-MM-2 was obtained from Deutsche Sammlung von Microorganismen und Zellkulturen. Cell lines were maintained in RPMI 1640 (Invitrogen) supplemented with 2 mmol/L L-glutamine, 10% FCS, and 50 μg/mL gentamicin (Invitrogen) under standard conditions (humidified atmosphere, 95% air, 5% CO_2, 37°C).

Ceramide Analyses HPLC-MS/MS

After treatment, samples were frozen at −80°C and transferred to the Lipidomics Core Facility at Medical University of South Carolina. Three lipids were measured by HPLC-MS/MS as described earlier (50).

Phosphate Assay

Phospholipids were extracted according to Bligh and Dyer (51). The samples and phosphate standards made of NaH_2PO_4 were washed in washing buffer (10 N H_2SO_4/70% $HClO_4$/H_2O) at 160°C overnight. Thereafter, 900 μL water, 500 μL of 9% ammonium molybdate, and 200 μL of 9% ascorbic acid were added to each sample followed by incubation at 45°C for 30 min. The amount of lipid phosphate was determined by measuring absorption at 590 nm.

Radioactive Lipid Analysis

Rec-1 cells were resuspended in AIM-V medium containing 2 μCi [^{3}H]palmitic acid to a concentration of 2 million/mL. After 12 h, cells were washed in PBS and treated with 10 μmol/L R-MA with or without pretreatment with inhibitors in fresh AIM-V medium.

Cells were harvested and washed in cold PBS three times. Subsequently, cells were dissolved in 50 μL PBS and the suspension was added to 1 mL methanol/$CHCl_3$ (1:2). To extract the lipids, 1 mL water was added to the samples that were centrifuged for 20 min at 4°C to attain two distinct phases. The lower phase containing the lipids was dried by SpeedVac for 45 min. Lipids were resuspended in 50 μL chloroform/methanol (2:1). The lipid samples were loaded onto a 60 Å silica TLC plate (Schleicher & Schnell) prewashed in acetone. The TLC plate was run for 45 min in a solvent system for ceramide (90 mL ethyl acetate/50 mL ocanoic acid/20 mL acetic acid) and then dried followed by treatment three times with ^{3}H enhancer spray. The plate was then developed for 48 h at −80°C. To quantify [^{3}H]ceramide, the area of interest was scraped into 3.5 mL scintillation fluid and analyzed by liquid scintillation. [^{3}H]ceramide was normalized to total ^{3}H-labeled cells loaded per lane. Treated samples were compared with vehicle-treated control.

RNA Isolation

Total RNA was prepared using Qiagen RNA purification system as directed by the supplier (Qiagen). The samples were treated with Turbo DNase Kit to eliminate genomic DNA (Ambion).

cDNA Synthesis and Quantitative Real-time PCR

First-strand cDNA synthesis was carried out according to the protocol for Omniscript Reverse Transcription (Qiagen). RNA (1 μg) was used in the reactions for real-time PCR. The Beacon Designer 3 program (Biosoft International) was employed for design of primers (see Table 1). Primers were synthesized by Integrated DNA Technologies. The quantification of CerS compared with β-actin was carried out with an iCycler iQ (Bio-Rad Laboratories). The iCycler iQ reaction detection system software from the same company was used for data analysis. cDNA was amplified using the qPCR Kit Platinum SYBR Green qPCR SuperMix-UGD with FITC (Invitrogen) according to the manufacturer's instructions. The samples were divided into triplicates in a 96-well PCR plate (Abgene) and run at 95°C for 10 min followed by 40 cycles, each cycle consisting of 15 s at 95°C and 1 min at 55°C. Threshold (Ct) cycle numbers were obtained from amplification of primers (Table 1). ΔCt values were calculated by subtracting the Ct value of β-actin from the Ct value of primers for the genes of interest. The relative fold increase of the genes of interest was calculated as follows. The ΔCt for controls and treated samples was first determined. The ΔCt value was calculated by subtracting the Ct value for housekeeping control from the Ct value for the gene of interest. The relative fold increase of genes of

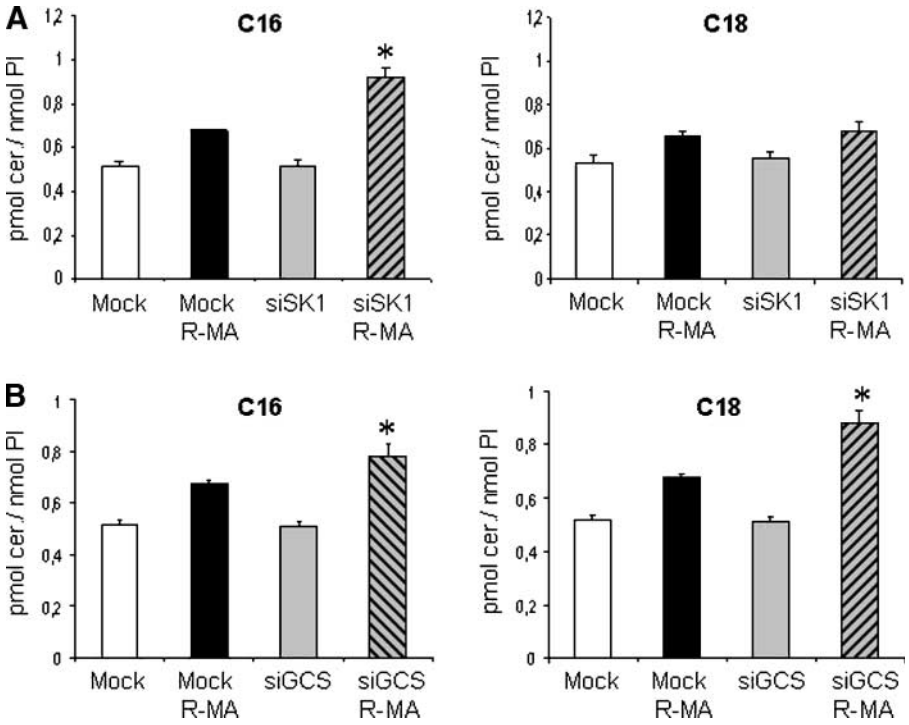

FIGURE 11. Effects of inhibition of ceramide metabolism in combination with cannabinoid treatment on accumulation of C_{16} and C_{18}. Rec-1 cells transfected with siRNA against (**A**) SK-1 or (**B**) GCS for 24 h were subsequently treated with 10 μmol/L R-MA for 12 or 24 h after transfection. After treatment (see below), cells were prepared for measurement of ceramide using HPLC-MS/MS as described in Materials and Methods. The masses of the ceramide subspecies C_{16} and C_{18} were normalized to lipid phosphate. One of two individually performed experiments. *, $P < 0.05$, agonist-treated cells with and without siRNA were compared (Kruskal-Wallis analysis).

interest was calculated by the equation: relative fold increase = $2^{-\Delta\Delta Ct}$. To use this calculation, the PCR efficiencies of the target and control assays must be similar. This was achieved by adjusting primer concentrations. The criterion for using the ΔCt method was fulfilled because by graphing serial dilutions of input cDNA of a random sample against ΔCt values (genes of interest − β-actin), the slope of the line was <<0.1 (data not shown).

Cell Death ELISA

Cell Death ELISA (Roche) is a quantitative sandwich ELISA that detects histone and intranucleosomal DNA fragmentation by binding to two different monoclonal antibodies. It allows specific determination of mononucleosomes and oligonucleosomes in the cytoplasmic fraction in cell lysates. The anti-histone-biotin antibody binds to histones H1, H2A, H2B, H3, and H4. The Anti-DNA-POD antibody reacts with double- or single-stranded DNA in the cytoplasm. In brief, cells were washed and resuspended in AIM-V medium. After treatment (see individual experiments in Results), cells were harvested and lysed with lysis buffer (Roche). The cell lysate was allowed to bind to the enzyme immunoassay plate for 2 h together with immunoreagent containing anti-DNA-POD and anti-histone-biotin and incubation buffer. Thereafter, ABTS substrate (Roche) was added for 10 min. Adding stop solution terminated the reaction, and the absorption was determined at 405 nm.

Electroporation

The cells were split 2 days before the experiment to assure that they are in logarithmic phase during electroporation. On the day of electroporation, 5 million cells were resuspended in 100 μL Nucleofector solution C (Amaxa Biosystems)/sample. To the cell suspension, 20 nmol/L duplex siRNA was added. The sample was then electroporated using Amaxa Nucleofector Systems, program X-001 (Amaxa Biosystems). The electroporated cells were then resuspended in 2.5 mL preheated RPMI 1640 supplemented with 10% fetal bovine serum. Transfection efficiency was evaluated by quantitative PCR.

Table 1. Primer Sequences Used for Quantitative Real-time PCR

Target	Forward primer (5′-3′)	Reverse primer (5′-3′)
CerS1 variant 1	ACGCTACGCTATACATGGACAC	AGGAGGAGACGATGAGGATGAG
CerS1 variant 2	ACGCTACGCTATACATGGACAC	GGAGACGATGAGGATGAGAGTG
CerS2	CCGATTACCTGCTGGAGTCAG	GGCGAAGACGATGAAGATGTTG
CerS3	ACATTCCACAAGGCAACCATTG	CTCTTGATTCCGCCGACTCC
CerS4	CTTCGTGGCGGTCATCCTG	TGTAACAGCAGCACCAGAGAG
CerS5	GCCATCGGAATCAGGAC	GCCAGCACTGTCGGATGT
CerS6	GGGATCTTAGCCTGGTTCTGG	GCCTCCTCCGTGTTCTTCAG
β-actin	ACCTGACTGACTACCTCATGAAGA	GCGACGTAGCACAGCTTCTC

Cell Viability

Viability of cells treated with R-MA and various modulators of ceramide metabolism was determined by using the XTT kit (Roche Diagnostics) according to the manufacturer's instructions. Absorbance was measured at 490 nm.

Statistical Analysis

Quantitative Cell Death ELISA was evaluated using the Kruskal-Wallis test comparing control and treated cells. *P* values are presented in figure legends. The software Statistica (Statsoft) was used.

Disclosure of Potential Conflicts of Interest

No potential conflicts of interest were disclosed.

Acknowledgments

We thank Dr. Alicja Bielawska for helpful technical advice and comments regarding the article.

References

1. Ogretmen B, Hannun YA. Biologically active sphingolipids in cancer pathogenesis and treatment. Nat Rev Cancer 2004;4:604–16.

2. Pewzner-Jung Y, Ben-Dor S, Futerman AH. When do Lasses (longevity assurance genes) become CerS (ceramide synthases)?: insights into the regulation of ceramide synthesis. J Biol Chem 2006;281:25001–5.

3. Eto M, Bennouna J, Hunter OC, Lotze MT, Amoscato AA. Importance of C16 ceramide accumulation during apoptosis in prostate cancer cells. Int J Urol 2006; 13:148–56.

4. Kroesen BJ, Jacobs S, Pettus BJ, et al. BcR-induced apoptosis involves differential regulation of C16 and C24-ceramide formation and sphingolipid-dependent activation of the proteasome. J Biol Chem 2003;278:14723–31.

5. Kroesen BJ, Pettus B, Luberto C, et al. Induction of apoptosis through B-cell receptor cross-linking occurs via *de novo* generated C16-ceramide and involves mitochondria. J Biol Chem 2001;276:13606–14.

6. Koybasi S, Senkal CE, Sundararaj K, et al. Defects in cell growth regulation by C18:0-ceramide and longevity assurance gene 1 in human head and neck squamous cell carcinomas. J Biol Chem 2004;279:44311–9.

7. Gustafsson K, Christensson B, Sander B, Flygare J. Cannabinoid receptor-mediated apoptosis induced by *R*(+)-methanandamide and Win55,212-2 is associated with ceramide accumulation and p38 activation in mantle cell lymphoma. Mol Pharmacol 2006;70:1612–20.

8. Carracedo A, Gironella M, Lorente M, et al. Cannabinoids induce apoptosis of pancreatic tumor cells via endoplasmic reticulum stress-related genes. Cancer Res 2006;66:6748–55.

9. Blazquez C, Carracedo A, Salazar M, et al. Down-regulation of tissue inhibitor of metalloproteinases-1 in gliomas: a new marker of cannabinoid antitumoral activity? Neuropharmacology 2008;54:235–43.

10. Mizutani Y, Kihara A, Igarashi Y. LASS3 (longevity assurance homologue 3) is a mainly testis-specific (dihydro)ceramide synthase with relatively broad substrate specificity. Biochem J 2006;398:531–8.

11. Mizutani Y, Kihara A, Igarashi Y. Mammalian Lass6 and its related family members regulate synthesis of specific ceramides. Biochem J 2005;390:263–71.

12. Braun PE, Snell EE. Biosynthesis of sphingolipid bases. II. Keto intermediates in synthesis of sphingosine and dihydrosphingosine by cell-free extracts of *Hansenula ciferri*. J Biol Chem 1968;243:3775–83.

13. Geeraert L, Mannaerts GP, van Veldhoven PP. Conversion of dihydroceramide into ceramide: involvement of a desaturase. Biochem J 1997;327:125–32.

14. Modrak DE, Gold DV, Goldenberg DM. Sphingolipid targets in cancer therapy. Mol Cancer Ther 2006;5:200–8.

15. Alemany R, van Koppen CJ, Danneberg K, Ter Braak M, Meyer Zu Heringdorf D. Regulation and functional roles of sphingosine kinases. Naunyn Schmiedebergs Arch Pharmacol 2007;374:413–28.

16. Segui B, Andrieu-Abadie N, Jaffrezou JP, Benoist H, Levade T. Sphingolipids as modulators of cancer cell death: potential therapeutic targets. Biochim Biophys Acta 2006;1758:2104–20.

17. Maurer BJ, Melton L, Billups C, Cabot MC, Reynolds CP. Synergistic cytotoxicity in solid tumor cell lines between *N*-(4-hydroxyphenyl)retinamide and modulators of ceramide metabolism. J Natl Cancer Inst 2000;92:1897–909.

18. Taha TA, Osta W, Kozhaya L, et al. Down-regulation of sphingosine kinase-1 by DNA damage: dependence on proteases and p53. J Biol Chem 2004;279: 20546–54.

19. Bektas M, Jolly PS, Muller C, Eberle J, Spiegel S, Geilen CC. Sphingosine kinase activity counteracts ceramide-mediated cell death in human melanoma cells: role of Bcl-2 expression. Oncogene 2005;24:178–87.

20. Liu YY, Han TY, Yu JY, et al. Oligonucleotides blocking glucosylceramide synthase expression selectively reverse drug resistance in cancer cells. J Lipid Res 2004;45:933–40.

21. Sun YL, Zhou GY, Li KN, et al. Suppression of glucosylceramide synthase by RNA interference reverses multidrug resistance in human breast cancer cells. Neoplasma 2006;53:1–8.

22. Olshefski RS, Ladisch S. Glucosylceramide synthase inhibition enhances vincristine-induced cytotoxicity. Int J Cancer 2001;93:131–8.

23. Dijkhuis AJ, Klappe K, Jacobs S, et al. PDMP sensitizes neuroblastoma to paclitaxel by inducing aberrant cell cycle progression leading to hyperploidy. Mol Cancer Ther 2006;5:593–601.

24. Gouaze V, Liu YY, Prickett CS, Yu JY, Giuliano AE, Cabot MC. Glucosylceramide synthase blockade down-regulates P-glycoprotein and resensitizes multidrug-resistant breast cancer cells to anticancer drugs. Cancer Res 2005;65: 3861–7.

25. Flygare J, Gustafsson K, Kimby E, Christensson B, Sander B. Cannabinoid receptor ligands mediate growth inhibition and cell death in mantle cell lymphoma. FEBS Lett 2005;579:6885–9.

26. Geisler CH, Kolstad A, Laurell A, et al. Long-term progression-free survival of mantle cell lymphoma after intensive front-line immunochemotherapy with *in vivo*-purged stem cell rescue: a nonrandomized phase 2 multicenter study by the Nordic Lymphoma Group. Blood 2008;112:2687–93.

27. Miyake Y, Kozutsumi Y, Nakamura S, Fujita T, Kawasaki T. Serine palmitoyltransferase is the primary target of a sphingosine-like immunosuppressant, ISP-1/myriocin. Biochem Biophys Res Commun 1995;211:396–403.

28. Triola G, Fabrias G, Casas J, Llebaria A. Synthesis of cyclopropene analogues of ceramide and their effect on dihydroceramide desaturase. J Org Chem 2003;68:9924–32.

29. Soriano JM, Gonzalez L, Catala AI. Mechanism of action of sphingolipids and their metabolites in the toxicity of fumonisin B1. Prog Lipid Res 2005;44: 345–56.

30. Radin NS. Killing cancer cells by poly-drug elevation of ceramide levels: a hypothesis whose time has come? Eur J Biochem 2001;268:193–204.

31. Norris-Cervetto E, Callaghan R, Platt FM, Dwek RA, Butters TD. Inhibition of glucosylceramide synthase does not reverse drug resistance in cancer cells. J Biol Chem 2004;279:40412–8.

32. French KJ, Upson JJ, Keller SN, Zhuang Y, Yun JK, Smith CD. Antitumor activity of sphingosine kinase inhibitors. J Pharmacol Exp Ther 2006;318:596–603.

33. Herrera B, Carracedo A, Diez-Zaera M, Gomez del Pulgar T, Guzman M, Velasco G. The CB2 cannabinoid receptor signals apoptosis via ceramide-dependent activation of the mitochondrial intrinsic pathway. Exp Cell Res 2006;312: 2121–31.

34. Galve-Roperh I, Sanchez C, Cortes ML, del Pulgar TG, Izquierdo M, Guzman M. Anti-tumoral action of cannabinoids: involvement of sustained ceramide accumulation and extracellular signal-regulated kinase activation. Nat Med 2000;6:313–9.

35. Gomez del Pulgar T, Velasco G, Sanchez C, Haro A, Guzman M. *De novo*-synthesized ceramide is involved in cannabinoid-induced apoptosis. Biochem J 2002;363:183–8.

36. Pettus BJ, Kroesen BJ, Szulc ZM, et al. Quantitative measurement of different ceramide species from crude cellular extracts by normal-phase high-performance liquid chromatography coupled to atmospheric pressure ionization mass spectrometry. Rapid Commun Mass Spectrom 2004;18:577–83.

37. Pettus BJ, Baes M, Busman M, Hannun YA, Van Veldhoven PP. Mass spectrometric analysis of ceramide perturbations in brain and fibroblasts of mice and human patients with peroxisomal disorders. Rapid Commun Mass Spectrom 2004;18:1569–74.

38. Hanada K. Serine palmitoyltransferase, a key enzyme of sphingolipid metabolism. Biochim Biophys Acta 2003;1632:16–30.

39. Rabionet M, van der Spoel AC, Chuang CC, et al. Male germ cells require polyenoic sphingolipids with complex glycosylation for completion of meiosis: a link to ceramide synthase-3. J Biol Chem 2008;283:13357–69.

40. Gustafsson K, Wang X, Severa D, et al. Expression of cannabinoid receptors type 1 and type 2 in non-Hodgkin lymphoma: growth inhibition by receptor activation. Int J Cancer 2008;123:1025–33.

41. Blazquez C, Salazar M, Carracedo A, et al. Cannabinoids inhibit glioma cell

invasion by down-regulating matrix metalloproteinase-2 expression. Cancer Res 2008;68:1945–52.

42. Dbaibo GS, Kfoury Y, Darwiche N, et al. Arsenic trioxide induces accumulation of cytotoxic levels of ceramide in acute promyelocytic leukemia and adult T-cell leukemia/lymphoma cells through *de novo* ceramide synthesis and inhibition of glucosylceramide synthase activity. Haematologica 2007;92:753–62.

43. Bielawska A, Crane HM, Liotta D, Obeid LM, Hannun YA. Selectivity of ceramide-mediated biology. Lack of activity of erythro-dihydroceramide. J Biol Chem 1993;268:26226–32.

44. Stiban J, Fistere D, Colombini M. Dihydroceramide hinders ceramide channel formation: implications on apoptosis. Apoptosis 2006;11:773–80.

45. Tserng KY, Griffin RL. Ceramide metabolite, not intact ceramide molecule, may be responsible for cellular toxicity. Biochem J 2004;380:715–22.

46. Kraveka JM, Li L, Szulc ZM, et al. Involvement of dihydroceramide desaturase in cell cycle progression in human neuroblastoma cells. J Biol Chem 2007;282:16718–28.

47. Sarkar S, Maceyka M, Hait NC, et al. Sphingosine kinase 1 is required for migration, proliferation and survival of MCF-7 human breast cancer cells. FEBS Lett 2005;579:5313–7.

48. Carracedo A, Lorente M, Egia A, et al. The stress-regulated protein p8 mediates cannabinoid-induced apoptosis of tumor cells. Cancer Cell 2006;9:301–12.

49. Sarfaraz S, Adhami VM, Syed DN, Afaq F, Mukhtar H. Cannabinoids for cancer treatment: progress and promise. Cancer Res 2008;68:339–42.

50. Bielawski J, Szulc ZM, Hannun YA, Bielawska A. Simultaneous quantitative analysis of bioactive sphingolipids by high-performance liquid chromatography-tandem mass spectrometry. Methods 2006;39:82–91.

51. Bligh EG, Dyer WJ. A rapid method of total lipid extraction and purification. Can J Biochem Physiol 1959;37:911–7.